Catalysis Today 141 (2009) 367–373

Contents lists available at ScienceDirect

Catalysis Today

journal homepage: www.elsevier.com/locate/cattod

Photocatalytic cyclohexane oxidehydrogenation on sulphated MoO_x/γ-Al_2O_3 catalysts

Paolo Ciambelli [a,*], Diana Sannino [a], Vincenzo Palma [a], Vincenzo Vaiano [a], Roberto Saverio Mazzei [a], Pierre Eloy [b], Eric M. Gaigneaux [b]

[a] Department of Chemical and Food Engineering, University of Salerno, 84084 Fisciano (SA), Italy
[b] Unité de catalyse et chimie des matériaux divisés, Université catholique de Louvain, B-1348 Louvain-la-Neuve, Belgium

ARTICLE INFO

Article history:
Available online 16 December 2008

Keywords:
Cyclohexane
Cyclohexene
Photocatalytic oxidative dehydrogenation
Fluidized bed reactor
Preparation method
Sulphated catalysts

ABSTRACT

The photocatalytic oxidative dehydrogenation of cyclohexane on sulphated MoO_x/γ-Al_2O_3 catalysts has been studied in a two-dimensional fluidized bed photoreactor. The influence of Mo loading at similar sulphate content and the effect of catalyst preparation method have been investigated.

Considering the influence of Mo loading at similar sulphate content, the highest photoactivity at 2.4 SO_4 wt% was found at MoO_3 loading of 8 wt%. Selectivity to cyclohexene was 100%, irrespective of the Mo content.

At fixed MoO_x content, in particular at 50% of theoretical monolayer coverage, the preparation method of catalysts strongly affected the photocatalysts performances, showing in addition a slight decrease in selectivity to cyclohexene due to side-production of benzene. All the catalysts showed a similar equivalent band gap energy. Thermogravimetric analysis evidenced the presence of surface sulphate species of different thermal stabilities. A linear correlation of photoactivity with the surface sulphates amount of lower thermal stability has been found for all sub-monolayer MoO_x sulphated catalysts. The neighboring of surface sulphates to octahedral polymolybdate species appears to be a key parameter for the photoactivity of the catalysts.

The catalyst selectivity was related to surface acidity. Higher acidity resulted in increased cyclohexene dark adsorption and consequently in enhanced benzene formation.

1. Introduction

Light alkanes oxidative dehydrogenation (ODH) is an attractive route to obtain olefins as alternative to dehydrogenation and steam-cracking processes. The limitation to the industrial application of the ODH process is the low olefins selectivity [1], mostly due to alkenes strong adsorption on the catalyst surface and the high rate of consecutive deep oxidation of the desired products [2]. Alternatively, the selective photocatalytic oxidative dehydrogenation of paraffin emerged as innovative way to perform ODH since high selectivity could be achieved [3,4].

Semiconductor photocatalysts have been intensively studied and widely applied to environmental purification [5]. Recent research has focused the attention on the selective photooxidation of organic compounds under mild conditions by using molecular oxygen as oxidant [6–9]. Indeed, TiO_2 based catalysts would allow for alternative catalytic processes, since the reaction is promoted under ambient temperature and pressure [10-14]. In liquid phase it was reported that TiO_2 can effectively catalyze partial oxidation reactions as shown by Boarini et al. [13] for the photooxidation of cyclohexane to cyclohexanol and cyclohexanone. The solvent in the reaction medium and the irradiation wavelength on products yield have a strong influence on distribution and nature of reaction products [15,16]. Other useful photocatalysts for selective oxidation were reported. Polytungstates showed good activity in the photoinduced oxidation of numerous organic compounds [17–19]. Modification of TiO_2 [20] with surface-bonded iron porphyrins induced an increase of the monooxygenated products in the photooxidation of cyclohexane. Alumina-supported vanadium oxide exhibited specific photocatalytic performance in the oxidation of cyclohexane to produce cyclohexanone [21]. The most active catalyst formulation was 5 wt% of V_2O_5 supported on Al_2O_3 with respect to other supports like TiO_2, ZrO_2 and SiO_2.

* Corresponding author at: Dipartimento di Ingegneria chimica e alimentare, Università di Salerno, 84084 Fisciano (SA), Italy. Tel.: +39 089964151; fax: +39 089964057.
E-mail address: pciambelli@unisa.it (P. Ciambelli).

0920-5861/$ – see front matter © 2008 Elsevier B.V. All rights reserved.
doi:10.1016/j.cattod.2008.10.020

In gas phase photocatalysed reactions most of the organic compounds undergo complete oxidation on TiO_2. For example, the oxidation of propene and cyclohexane on TiO_2 [22] and on sulphated TiO_2 [3] resulted in very high selectivities to CO_2 (96.2% and 100%, respectively). However, we showed that benzene is selectively obtained from cyclohexane photooxidative dehydrogenation reaction on TiO_2 based catalysts modified by polymolybdates. First results were obtained in a gas–solid fixed bed reactor [3,4], while higher conversion and benzene yield were obtained in a two-dimensional fluidized bed reactor [23–25]. Moreover, the addition of sulphate to MoO_x/γ-Al_2O_3 catalysts was found to promote the selective mono-oxidative dehydrogenation of cyclohexane to cyclohexene [26]. An optimum in MoO_3 and SO_4 loading was found to be 8 and 2.4 wt%, respectively, and the decreasing of catalytic activity at higher sulphate loading was ascribed to MoO_x decoration by sulphates. However, the role of molybdate and sulphate on titania and alumina surface is still to be completely rationalized. In this study, the influence of the Mo loading and the effect of catalyst preparation method in the photooxidative dehydrogenation of cyclohexane were investigated using alumina as catalyst support.

2. Experimental

MoO_x/γ-Al_2O_3 catalysts were prepared by incipient wet impregnation of γ-Al_2O_3 (Puralox SBA 150, SASOL, 144 m^2/g) with different amounts of aqueous solutions of ammonium heptamolybdate (AHM), drying at 120 °C and calcination in air at 500 °C for 3 h. The samples were then sulphated by incipient wet impregnation at SO_4 nominal load of 2.4 wt% with an aqueous solution of ammonium sulphate (AS), drying at 120 °C and after calcined in air at 300 °C for 3 h. The catalysts were named as XMo2S (where X is MoO_3 nominal wt%). In order to elucidate the effect of the preparation method the sample containing 8 wt% MoO_3 and 2.4 wt% SO_4 was also prepared (i) by reversing the impregnation order, first with AS aqueous solution, then with AHM aqueous solution (2S8Mo) and (ii) by simultaneous AHM and AS impregnation ($8Mo2S_{sim}$). Calcination was carried out at 300 °C for 3 h in all cases. For comparison sulphated aluminas (XS, where X is SO_4 wt%) and unsulphated Mo-based alumina catalyst (8Mo) were also prepared as reported in [26].

Thermogravimetric analysis (TG–DTG–MS) was carried out in air flow with a thermoanalyzer (Q600, TA Instruments), on-line connected with a quadrupole mass spectrometer (Quadstar 422, Pfeiffer Vacuum) at heating rate of 10 °C/min in the range 20–1100 °C. Specific surface areas of calcined samples, pretreated at 180 °C for 2 h in He flow (99.9990%), were obtained by N_2 adsorption isotherm at −196 °C with a Costech Sorptometer 1040. XPS analyses were performed with a Kratos Axis Ultra spectrometer (Kratos Analytical – Manchester – UK) equipped with a monochromatised aluminium X-ray source (powered at 10 mA and 15 kV). The sample powders were pressed into small stainless steel troughs mounted on a multi-specimen holder. The pressure in the analysis chamber was around 10^{-6} Pa. The angle between the normal to the sample surface and the lens axis was 0°. The hybrid lens magnification mode was used with the slot aperture resulting in an analyzed area of 700 μm × 300 μm. The pass energy was set at 40 eV. In these conditions, the energy resolution gives a full width at half maximum (FWHM) of the Ag $3d_{5/2}$ peak of about 1.0 eV. Charge stabilization was achieved by using the Kratos Axis device. The following sequence of spectra was recorded: survey spectrum, C 1s, O 1s, Al 2p, S 2p, Mo 3d and C 1s again to check the stability of charge compensation in function of time and the absence of degradation of the sample during the analyses. The binding energies were calculated with respect to the C-(C,H) component of the C 1s peak fixed at 284.8 eV.

Also, thanks to the samples without Mo, constraints for the position and the width of S 2s peaks were determined and used for subtracting the S 2s contributions from each Mo peaks. Molar fractions were calculated using peak areas normalised on the basis of acquisition parameters, sensitivity factors provided by the manufacturer and the transmission function.

The spectra were decomposed with the CasaXPS program (Casa Software Ltd., UK) with a Gaussian/Lorentzian (70/30) product function after subtraction of a linear baseline. Although Mo $3d_{3/2}$ and Mo $3d_{5/2}$ peaks overlap S 2s peak, it was taken into account that the theoretical distance between Mo $3d_{3/2}$ and Mo $3d_{5/2}$ peaks is 3.13 eV and the area ratio is 2/3. Also, thanks to the sample without Mo, constraints for the position (232.2 ± 0.2 eV) and the width (3.0 ± 0.2 eV) of S 2s peaks were determined and used for subtracting the S 2s contributions from each Mo peaks. Molar fractions were calculated using peak areas normalised on the basis of acquisition parameters, sensitivity factors provided by the manufacturer and the transmission function.

Laser Raman spectra of powder samples were obtained in air with a Dispersive MicroRaman (Invia, Renishaw), equipped with 785 nm diode-laser, in the Raman shift range 100–2500 cm^{-1}.

The zero point charge (ZPC) of supports and catalysts was determined by mass titration according to Noh and Schwarz [27]. UV–vis reflectance spectra in the range 200–800 nm of powder bare catalysts were recorded by a PerkinElmer spectrometer Lambda 35 using a RSA-PE-20 reflectance spectroscopy accessory (Labsphere Inc., North Sutton, NH). The reflectance data were reported as the $F(R_\infty)$ value from Kubelka-Munk theory vs. the wavelength. Assuming that the dispersed MoO_x phase behaves in light absorption in a similar way to a direct gap semiconductor, equivalent band gap determinations were performed by plotting $[F(R_\infty)^* h\nu]^2$ vs. $h\nu$ (eV) and calculating the x intercept of a line passing through $0.5 < F(R_\infty) < 0.8$ [28].

Catalytic tests were carried out feeding 1000 ppm cyclohexane, 1500 ppm oxygen and 1600 ppm water in N_2 (total flow rate: 830 (stp) cm^3/min). Cyclohexane and water were vaporised by two temperature-controlled saturators. The gas flow rates were measured and adjusted by mass flow controllers (Brooks Instrument). The reactor inlet or outlet gases were fed to an on-line quadrupole mass detector (MD800, ThermoFinnigan) and a continuous CO-CO_2 NDIR analyzer (Uras 10, Hartmann & Braun). The characteristics of the fluidized bed reactor are reported in [26]. The reactor was illuminated by four UV light sources (EYE MERCURY LAMP, 125W) with spectrum emission centred at 365 nm in a dark box. The light intensity entering at reactor walls (40 × 230 mm) was measured by an UV meter and equal to 10 mW/cm^2. The reactor temperature was set and controlled at 120 °C by a PID temperature controller connected to a heating system. In order to achieve fluidization conditions, 14 g of catalyst (grain size: 25–38 μm) and 63 g of α-Al_2O_3 (Aldrich, 10 m^2/g) with Sauter average diameter of 50 μm and bulk density equal to 3970 kg/m^3 were mixed and loaded to the photoreactor. No positional fractioning of two components was observed. Typical photocatalytic test started feeding the reaction gaseous mixture to the photoreactor at reaction temperature in dark. After the complete adsorption of cyclohexane on the catalyst surface corresponding to the restoring of initial hydrocarbon concentration, lamps were switched on. With the lamps off, no reaction products were observed either during the cyclohexane dark adsorption or after that cyclohexane adsorption equilibrium was reached.

Table 1
Catalysts and their characteristics.

Catalyst	MoO_3, wt%	SO_4, wt%	SO_4,[a] wt%	Specific surface area, m^2/g	MoO_3 surface density, μmol/m^2	SO_4 surface density, μmol/m^2	Equivalentband gap energy, eV
2S	0	2.4	2.5	135	0	1.9	–
6S	0	7.2	6.8	–	0	–	–
8Mo2S	8	2.4	2.6	135	4.1	2.0	3.4
10Mo2S	10	2.4	2.5	133	5.2	1.9	3.2
16Mo2S	16	2.4	2.5	126	8.8	2.1	3.3
2S8Mo	8	2.4	2.4	135	4.1	1.8	3.4
$8Mo2S_{sim}$	8	2.4	2.6	139	4.0	1.9	3.4

[a] Evaluated by TG-MS analysis.

3. Results and discussion

3.1. Catalyst characterization

The list of catalysts investigated and their composition is reported in Table 1. Specific surface areas are similar to the parent alumina (144 m^2/g) and sulphated alumina (135 m^2/g) [26]; a slight decrease was observed for only 16Mo2S catalyst. MoO_3 surface density was estimated from its nominal load; assuming that 15.8 wt% correspond to the formation of one MoO_3 monolayer [29], catalysts with coverages corresponding to 50, 63 and 101% of a monolayer were thus prepared.

TG–DTG curves coupled to MS analyses (not reported) for Mo-based catalysts are shown in Fig. 1 and allow to distinguish four main weight loss steps, two due to water ($m/z = 18$) in the range 20–220 °C and 250–520 °C, a third complex step of decomposition of sulphates [26], and a further fourth weight loss above 800 °C due to Mo oxides sublimation [30]. The sulphate content, as calculated by considering the evolution of SO_2 in the range 500–800 °C is reported in Table 1. For comparison, TG–DTG curves of sulphated γ-alumina are reported in Fig. 1. DTG curve of 2S shows a high temperature peak centred at 920 °C. At higher sulphate load, the thermal window of surface sulphates decomposition enlarges with a downshift of the decomposition onset temperature. Additional convoluted DTG peaks with maxima at about 870, 761 and 700 °C are individuated. On a sulphated alumina, three sulphate weight losses, with DTG peaks at 650, 810, and 950 °C were described in [30]. These species have been attributed to multilayer sulphate, $Al_2(SO_4)_3$, and surface sulphates, respectively [31]. It must be noted that for our sulphated aluminas and catalysts the intense DTG peak at about 800 °C is not detected. Therefore, taking into account the SO_4 content, we can conclude that our samples only contain surface sulphates. They can be attributed to monoxo sulphates linked to three Al^{3+}, or dioxo sulphates bounded to two Al^{3+}, acid sulphates bi- or mono-oxygen bonded, or an SO_3 group linked to an Al–O pair site [32,33]. Sulphates with a high number of links to the surface are expected to be thermally more stable. The presence of MoO_x species causes a decrease in sulphates decomposition temperature (Fig. 1) showing that sulphates and polymolybdates compete on the same alumina sites. Irrespective of the preparation method, polymolybdates occupy the alumina sites of high thermal stability. The consequence is thus that the sulphates coordination to those sites is hindered, thus making that the sulphates are forced to different coordinations of lower thermal stability. As another consequence, when the Mo load increases, as in the case of 8Mo2S, 10Mo2S and 16Mo2S, sulphates loss occurs at lower temperatures. The sulphates decomposition thermal window for all Mo-based catalysts is detailed in Fig. 2. DTG curves of 8Mo2S can be decomposed into two peaks, centred respectively at about 670 °C and 750 °C. $8Mo2S_{sim}$ and 2S8Mo catalysts show three DTG peaks centred at 699 °C, 759 °C, 827 °C and at 712 °C, 785 °C, and 843 °C, respectively, evidencing the presence of a different distribution of surface sulphates induced by changing the preparation sequence. Similar values of DTG peaks temperatures, centred at 680 °C,

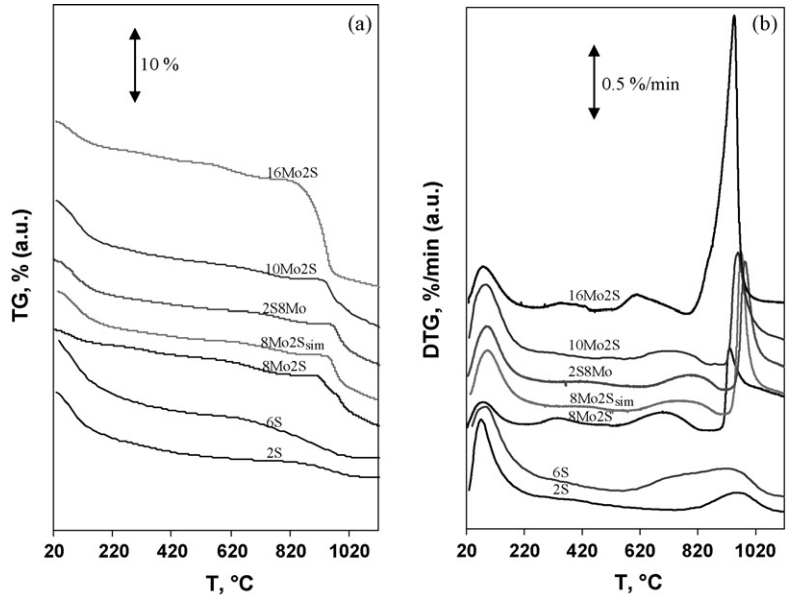

Fig. 1. TG (a) and DTG (b) curves of 2S, 6S, 8Mo2S, $8Mo2S_{sim}$, 2S8Mo, 10Mo2S and 16Mo2S catalysts.

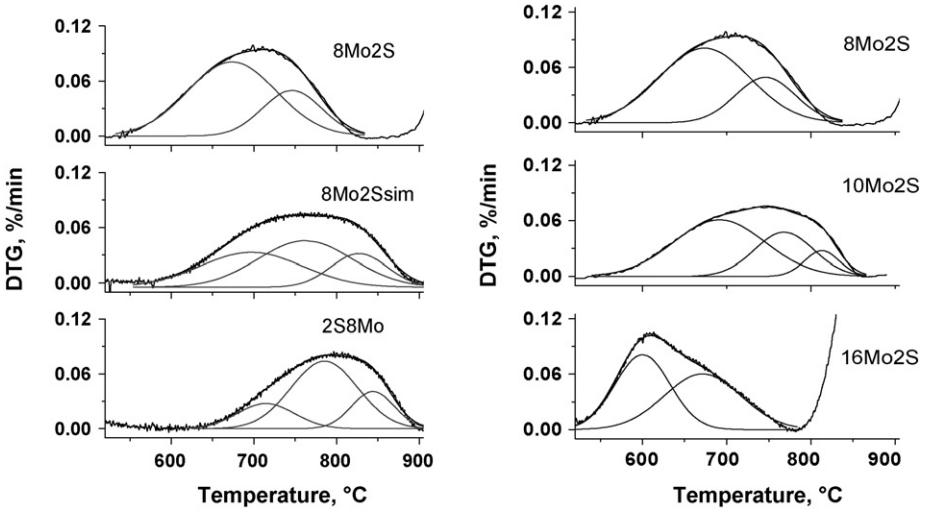

Fig. 2. DTG curves of 8Mo2S, 10Mo2S, 16Mo2S, 8Mo2S_{sim} and 2S8Mo catalysts.

770 °C and 813 °C were observed for 10Mo2S. On 16Mo2S, the highest temperature peaks disappear, as sulphate loss ends at about 720 °C (as verified by MS signals, not shown), but a new low temperature peak at 600 °C is observed in addition to the DTG peak at 670 °C. This fourth sulphate species results in the lowest thermal stability; its formation is likely induced by the high surface occupation by Mo, which exceeds MoO_3 monolayer capacity because of the high MoO_3 content.

XPS analyses showed photoemission peaks due to O 1s (531.4 eV), Al 2p (74.7 eV), S 2p (169.5 eV) and Mo 3d (233 eV and 231.7 eV) for all the samples. No significant differences in the binding energies for the elements were found. In Table 2 O/Al, Mo/Al, S/Al surface atomic ratios are reported. For the catalysts prepared by changing the preparation sequence, the surface concentration of Mo was almost the same, suggesting that no decoration of MoO_x species by sulphate occurred, as was evidenced at high SO_4 contents [26]. However, 8Mo2S catalyst shows the highest S exposure with respect to 2S8Mo and 8Mo2S_{sim}. The values of surface Mo/Al atomic ratios grow linearly with Mo loading up to 10 MoO_3 wt%. It must be considered that part of the alumina surface is covered by sulphate species, so MoO_3 segregation occurs at lower MoO_3 content.

The Raman spectra of all samples are displayed in Fig. 3. The Mo=O stretching band at 960–966 cm^{-1}, characteristic of octahedral polymolybdenyl species [29], is present on 8Mo2S, 2S8Mo and 8Mo2S_{sim} without significant differences due to the preparation method [34]. For 10Mo2S, a wider band with maximum at about 987 cm^{-1}, indicates a higher degree of polymerization for Mo surface species. The contribution of sulphate coordinated to the surface is expected at 984 cm^{-1} [26]. This, in addition to the quite low sulphate content of all catalysts, results in a difficult evaluation analysis of the sulphate species by this technique. On 16Mo2S, formation of MoO_3 crystallites was clearly detected, as shown by the presence of bulk molybdena bands at 819 and 995 cm^{-1} [35].

Table 2
Surface atomic ratios.

	8Mo2S	10Mo2S	16Mo2S	2S8Mo	8Mo2S_{sim}
O/Al	1.64	1.67	1.65	1.67	1.63
C/Al	0.28	0.33	0.30	0.29	0.28
Mo/Al	0.043	0.048	0.058	0.042	0.043
S/Al	0.021	0.019	0.023	0.017	0.017

UV–vis DRS spectra are reported in Fig. 4. As previously reported [26], both alumina and sulphated alumina show no significant absorptions. On both 8Mo2S and 8Mo2S_{sim}, two main bands at about 257 and 297 nm due to octahedrally coordinated polymolybdena species are visible [36]. For 2S8Mo the UV bands are lower and broader than for 8Mo2S and 8Mo2S_{sim} catalysts. Neither the different Mo loading nor the preparation methods induce any difference in the equivalent band gap energy values (Table 1). By increasing Mo loading, the two bands found for 8Mo2S catalyst shift to higher wavelengths and the overall absorption decreases and gets wider. For 10Mo2S, a shoulder at about 250 nm, attributed to octahedrally coordinated Mo^{6+} [36] appears. Moreover a shoulder at about 320 nm is detected on 16Mo2S indicating the presence of MoO_3 on the catalysts [37].

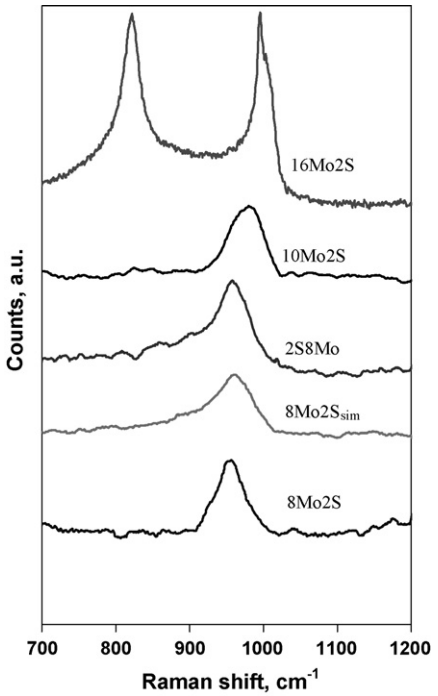

Fig. 3. Raman spectra of 8Mo2S, 10Mo2S, 16Mo2S, 2S8Mo and 8Mo2S_{sim} catalysts.

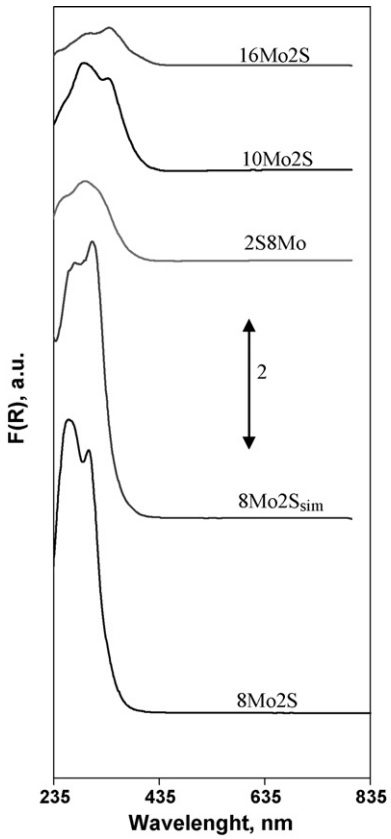

Fig. 4. UV–vis DRS spectra 8Mo2S, 10Mo2S, 16Mo2S, 2S8Mo and 8Mo2S$_{sim}$ catalysts.

3.2. Photocatalytic tests

A series of control tests were previously carried out in order to verify that the observed cyclohexane conversion was really due to a heterogeneous photocatalytic reaction. As previously found, both on titania [3,4] and alumina based catalysts [26] no activity was detected in the dark. In addition, α-Al_2O_3 and γ-Al_2O_3 alone, sulphated Al_2O_3, and unsulphated MoO_x/γ-Al_2O_3 (8Mo) catalysts did not show any photoactivity [26]. Photocatalytic tests under irradiation of 8Mo2S, 10Mo2S and 16Mo2S evidenced that the only detected product of cyclohexane conversion was cyclohexene, thus corresponding to 100% selectivity. The catalytic behaviors as a function of irradiation time (not reported) are similar to that reported in [26]. Cyclohexane consumption rate and cyclohexene formation rates as functions of Mo content are shown in Fig. 5. They had a maximum value of about 18 μmol h^{-1} g^{-1} at a Mo surface density of about 4 μmol/m^2, and then they decreased with molybdenum content. The negligible photocatalytic activity of 16Mo2S can be attributed to the segregation of MoO_3 crystallites (whose presence was evidenced by XPS analyses, Raman and UV–vis DRS analyses) that are inactive with respect to the photocatalytically active surface molybdates present at sub-monolayer Mo content. The apparent quantum yield for 8Mo2S sample was calculated as the ratio between the number of cyclohexane molecules reacted per second and the number of photons entering the reactor per second. The value is 1.2%, which is in the range 1–2% reported for the photocatalytic partial oxidation of cyclohexane in liquid phase [16].

Photocatalytic activity results on 8Mo2S, 8Mo2S$_{sim}$ and 2S8Mo catalysts are reported in Fig. 6. Cyclohexane conversion reached the highest value (11% after 50 min) on 8Mo2S with respect to

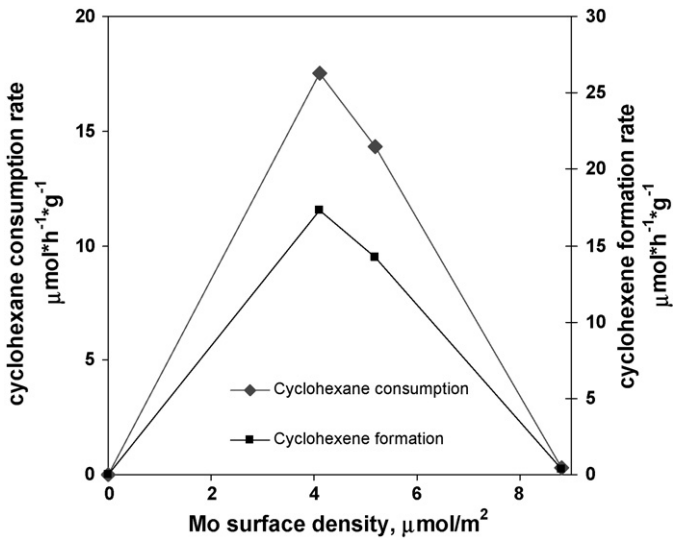

Fig. 5. Cyclohexane consumption and cyclohexene formation rate on 2S. 8Mo2S, 10Mo2S and 16Mo2S catalysts as a function of Mo surface density.

8Mo2S$_{sim}$ (about 6%) and 2S8Mo (about 2%). While on 8Mo2S sample cyclohexene was the only product detected in the gas phase (see above), a different products distribution was observed on 8Mo2S$_{sim}$ and 2S8Mo: namely, together with cyclohexene, benzene was also produced (Fig. 6b). Cyclohexene was formed simultaneously to cyclohexane conversion after that the lamp was turned on, reaching a maximum concentration value after about 7 min. Then it decreased to steady state values (110, 58 and 13 ppm on 8Mo2S, 8Mo2S$_{sim}$ and 2S8Mo, respectively) after about 30 min. Benzene started to appear after about 5 min under illumination and its steady state value was about 2 ppm on 8Mo2S$_{sim}$ and 7 ppm on 2S8Mo. These behaviors evidenced that

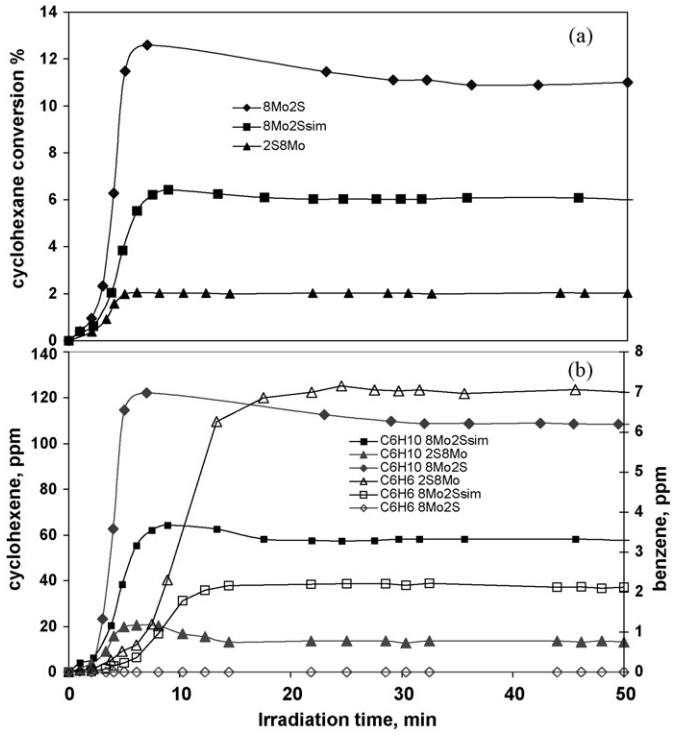

Fig. 6. Cyclohexane conversion (a), cyclohexene and benzene outlet concentration (b) on 8Mo2S, 8Mo2S$_{sim}$ and 2S8Mo as function of irradiation time.

Table 3
Photocatalytic performances comparison of 8Mo2S, 8Mo2S$_{sim}$ and 2S8Mo catalysts.

Catalyst	Cyclohexane conversion, %	Cyclohexene selectivity, %	Benzene selectivity, %	Carbon dioxide selectivity, %
8Mo2S	11	0	100	0
8Mo2S$_{sim}$	6	88	12	0
2S8Mo	2	91	9	0

Table 4
Dark adsorption data of cyclohexane and cyclohexene and ZPC values for 8Mo2S, 8Mo2Ssim 2S8Mo, 10Mo2S and 16Mo2s catalysts.

Catalyst	Cyclohexane, μmol/m^2	Cyclohexene, μmol/m^2	ZPC, pH unit
8Mo2S	0.22	0.017	4.62
8Mo2S$_{sim}$	0.13	0.020	4.08
2S8Mo	0.04	0.024	4.49
10Mo2S	0.19	–	4.01
16Mo2S	0.02	–	4.40

cyclohexene can be considered as an intermediate in the course of the formation of benzene from cyclohexane.

In Table 3 the catalytic performances of 8Mo2S, 8Mo2S$_{sim}$ and 2S8Mo are summarized. It is evident that the preparation method influenced both conversion and selectivity of the photocatalysts. The catalysts photoactivity is not attributable to catalysts acidity (Table 4). Indeed although 8Mo2S has the lowest acidity and highest activity, no further correlation involving all the other samples can be found. The values of ZPC (Table 4) can instead explain the different selectivity to benzene or cyclohexene for 8Mo2S, 2S8Mo and 8Mo2S$_{sim}$ samples. The amount of adsorbed cyclohexene in dark conditions increased with the decrease of ZPC values (Table 4), indicating that the raise of catalysts acidity enhances the adsorption of cyclohexene on the catalyst surface, thus favouring its conversion to benzene. On TiO_2 based catalysts we proposed [38] a photoreaction mechanism involving photo-excited octahedral molybdate surface species able to perform the oxidative dehydrogenation of adsorbed cyclohexane through hydrogen abstraction to form cyclohexene, which is afterwards oxidehydrogenated in series to benzene. Photoreduced molybdates can be reoxidized by reactive oxygen species [38]. Adsorption of cyclohexane appears to depend on the kind of sulphate species present at the surface.

It is worth to note that in the absence of sulphate MoO_x/Al_2O_3 catalysts are not photoactive [26]. As pointed out previously [30], the presence of sulphate can give higher photoefficiency, attributed to energy required to excite the electrons from the valence to the conduction band (E_g). Moreover, sulphate can limit electron–hole pair recombination owing its electron withdrawing properties. No differences were observed between the equivalent band gap energies of the catalysts (Table 1). Surface sulphates can also participate into the reoxidation step of the surface octahedrally coordinated polymolybdates. Further hypothesis involves the promotion of hydrogen abstraction by $^{-}SO_3H$ from adsorbed cyclohexane molecules, thanks to its acid properties [38]. It is known that sulphated aluminas possess thermally stable surface sulphate groups able to enhance the adsorption of light alkanes and subsequent low temperature C–H activation [39]. As a consequence, sulphate species should be neighbored to polymolybdates, likely forming a "dual site" for the conversion of quite large molecule like cyclohexane. We assume that acid sulphates mono-oxygen bonded, like $^{-}SO_3H$ groups, whose presence is suggested by the mild temperature conditions of photocatalytic tests, and the presence of water in the reaction stream, could help in hydrocarbon hydrogen abstraction. After activation, hydrocarbon could be photocatalytically converted by vicinal surface photoactive polymolybdates, whose mean nuclearity ranges around 7–8 on the most active catalysts.

Excluding the fourth sulphate species, formed only when the samples have Mo content exceeding the monolayer coverage, a linear correlation between cyclohexane consumption rate and the amount of sub-monolayer surface sulphate species of lower thermal stability (LTS) for 8Mo2S, 8Mo2S$_{sim}$ and 2S8Mo was found, strongly supporting the previous hypothesis. The correlation is even more strongly supported by the value of 10Mo2S relevant rate, located on the same straight line (Fig. 7a). Noticeably,

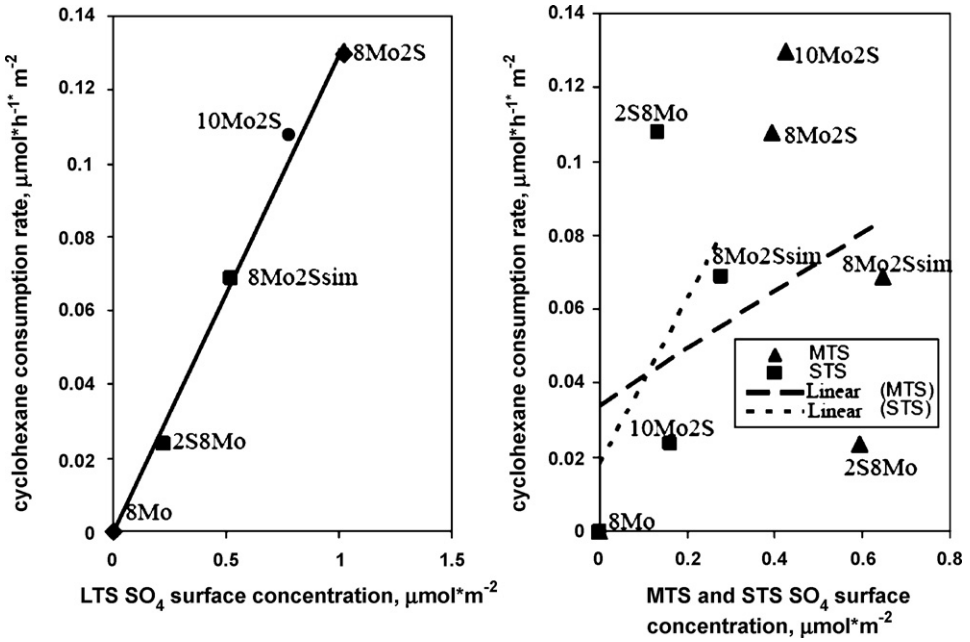

Fig. 7. (a) Cyclohexane consumption rate as a function of LTS SO_4 surface concentration for 8Mo, 8Mo2S, 2S8Mo, 8Mo2Ssim (■) and 10Mo2S (●) catalysts and (b) cyclohexane consumption rate as a function of MTS and STS SO_4 surface concentration for 8Mo, 8Mo2S, 2S8Mo, 8Mo2Ssim and 10Mo2S catalysts.

no correlation was found for surface sulphate of medium thermal stability (MTS) and strong thermal stability (STS) as shown in Fig. 7b.

4. Conclusions

Photocatalytic oxidative dehydrogenation of cyclohexane was studied on sulphated MoO_x/γ-Al_2O_3 catalysts. 100% selectivity to cyclohexene was obtained by sulphation of MoO_x/γ-Al_2O_3 catalysts at about 50% of MoO_x monolayer coverage. The preparation method strongly affects the catalyst performances. The selectivity to benzene depends on the catalyst acidity, as the latter favours the cyclohexene adsorption and thus its conversion to benzene. A linear correlation of photoactivity with the amount of surface sulphate species of lower thermal stability has been found for all sub-MoO_x monolayer catalysts. The neighboring of surface sulphates to octahedral polymolybdates appears to be a key parameter for the photoactivity of the catalysts.

References

[1] H.H. Kung, Adv. Catal. 40 (1994) 1.
[2] T.C. Watling, G. Deo, K. Seshan, I.E. Wachs, J.A. Lercher, Catal. Today 28 (1996) 139.
[3] P. Ciambelli, D. Sannino, V. Palma, V. Vaiano, Stud. Surf. Sci. Catal. 155 (2005) 179.
[4] P. Ciambelli, D. Sannino, V. Palma, V. Vaiano, Catal. Today 99 (2005) 143.
[5] A. Fujishima, T.N. Rao, D.A. Tryk, J. Photochem. Photobiol. C: Photochem. Rev. 1 (2000) 1.
[6] S. Ito, A. Kunai, H. Okada, K. Sasaki, J. Org. Chem. 53 (1988) 296.
[7] T. Ohtani, S. Nishiyama, S. Tsuruya, M. Masai, J. Catal. 155 (1995) 158.
[8] N. Komiya, T. Naota, Y. Oda, S. Murahashi, J. Mol. Catal. A 117 (1997) 21.
[9] I. Yamanaka, M. Katagiri, S. Takenaka, K. Otsuka, Stud. Surf. Sci. Catal. 130 (2000) 809.
[10] Y. Shimamura, H. Misawa, T. Oguchi, T. Kanno, H. Sakuragi, K. Tokumaru, Chem. Lett. (1983) 1691.
[11] W. Mu, J. Herrmann, P. Pichat, Catal. Lett. 3 (1989) 73.
[12] P. Pichat, Catal. Today 19 (1994) 313.
[13] P. Boarini, V. Carassiti, A. Maldotti, R. Amadelli, Langmuir 14 (1998) 2080.
[14] M.A. Gonzalez, S.G. Howell, S.K. Sikdar, J. Catal. 183 (1999) 159.
[15] L. Cerveny, V. Ruzicka, Adv. Catal. 30 (1981) 335.
[16] P. Du, J.A. Moulijn, G. Mul, J. Catal. 238 (2006) 342.
[17] R. Neumann, M. Dahan, Nature 388 (1997) 353.
[18] L.P. Ermolenko, C. Giannotti, J. Chem. Soc. Perkin Trans. 1205 (1996).
[19] A. Molinari, R. Amadelli, V.V. Carassiti, A. Maldotti, Eur. J. Inorg. Chem. 91 (2000).
[20] E. Polo, R. Amadelli, V. Carassiti, A. Maldotti, Inorg. Chim. Acta Lett. 192 (1992) 1.
[21] K. Teramura, T. Tanaka, T. Yamamoto, T. Funabiki, J. Catal. Mol. A: Chem. 165 (2001) 299.
[22] H. Yoshida, C. Murata, T. Hattori, J. Catal. 194 (2000) 364.
[23] P. Ciambelli, V. Palma, D. Sannino, S. Vaccaro, V. Vaiano, Stud. Surf. Sci Catal. 172 (2007) 453.
[24] V. Vaiano, PhD Thesis, University of Salerno, Italy, March 2006.
[25] P. Ciambelli, D. Sannino, V. Palma, V. Vaiano, Italian patent pending SAA2008000012.
[26] P. Ciambelli, D. Sannino, V. Palma, V. Vaiano, P. Eloy, F. Dury, E.M. Gaigneaux, Catal. Today 128 (2007) 251.
[27] J. Noh, J. Schwarz, J. Colloid Interface Sci. 130 (1989) 157.
[28] C. Anderson, A.J. Bard, J. Phys. Chem. B 101 (1997) 2611.
[29] I. Wachs, Catal. Today 27 (1996) 437.
[30] P. Ciambelli, D. Sannino, V. Palma, V. Vaiano, Int. J. Photoenergy, (2008) doi:10.1155/2008/258631.
[31] T. Yang, T. Chang, C. Yeh, J. Mol. Catal. 115 (1997) 339.
[32] M. Waqif, O. Saur, J.C. Lavalley, S. Perathoner, G. Centi, J. Phys. Chem. 95 (1991) 4051.
[33] M.B. Mitchell, M.G. White, J. Phys. Chem. 100 (1996) 7550.
[34] C.P. Cheng, G.L. Schrader, J. Catal. 60 (1979) 276.
[35] C. Martin, M.J. Martin, V. Rives, Stud. Surf. Sci. Catal. 72 (1992) 415.
[36] M. Cheng, F. Kumata, T. Saito, T. Komatsu, T. Yashima, Appl. Catal. A: Gen. 183 (1999) 199.
[37] A. Duan, G. Wan, Z. Zhao, C. Xu, Y. Zheng, Y. Zhang, T. Dou, X. Bao, K. Chung, Catal. Today 119 (2007) 13.
[38] P. Ciambelli, D. Sannino, V. Palma, V. Vaiano, R.I. Bickley, Appl. Catal. A: Gen. 349 (2008) 140.
[39] D.E. Gawthrope, A.F. Lee, K. Wilson, Phys. Chem. Chem. Phys. 6 (2004) 3907.